Published January 2, 2012



# The vesicular SNARE Synaptobrevin is required for Semaphorin 3A axonal repulsion

Kathleen Zylbersztejn,[1,2] Maja Petkovic,[1,2] Andrea Burgo,[1,2] Marie Deck,[3] Sonia Garel,[3] Séverine Marcos,[4] Evelyne Bloch-Gallego,[4] Fatiha Nothias,[5] Guido Serini,[6,7] Dominique Bagnard,[8] Thomas Binz,[9] and Thierry Galli[1,2]

[1]University Paris Diderot, Sorbonne Paris Cité, Jacques Monod Institute, Centre National de la Recherche Scientifique UMR7592, Program in Development and Neurobiology, Paris, 75013 France
[2]"Membrane Traffic in Neuronal and Epithelial Morphogenesis," Institut National de la Santé et de la Recherche Médicale ERL U950, Paris, 75013 France
[3]Institut de Biologie de l'École Normale Supérieure, Ecole Normale Supérieure, Institut National de la Santé et de la Recherche Médicale U1024, Centre National de la Recherche Scientifique UMR8197, Paris, 75005 France
[4]Cochin Institute, University Paris Descartes, Centre National de la Recherche Scientifique UMR8104, Department in Genetic and Development, Institut National de la Santé et de la Recherche Médicale U567, Paris, 75005 France
[5]"Axon Regeneration and Growth," Physiopathologie des Maladies du Système Nerveux Central, Institut National de la Santé et de la Recherche Médicale U952, Centre National de la Recherche Scientifique UMR 7224, University Pierre and Marie Curie, Paris, 75005 France
[6]Laboratory of Cell Adhesion Dynamics, Institute for Cancer Research and Treatment, Candiolo, 10060 Italy
[7]Department of Oncological Sciences, University of Torino School of Medicine, Candiolo, 10060 Italy
[8]Institut National de la Santé et de la Recherche Médicale U682, Strasbourg, 67000 France
[9]Institute of Biochemistry, Medizinische Hochschule Hannover, Hannover, 30001 Germany

Attractive and repulsive molecules such as Semaphorins (Sema) trigger rapid responses that control the navigation of axonal growth cones. The role of vesicular traffic in axonal guidance is still largely unknown. The exocytic vesicular soluble *N*-ethylmaleimide sensitive fusion protein attachment protein receptor (SNARE) Synaptobrevin 2 (Syb2) is known for mediating neurotransmitter release in mature neurons, but its potential role in axonal guidance remains elusive. Here we show that Syb2 is required for Sema3A-dependent repulsion but not Sema3C-dependent attraction in cultured neurons and in the mouse brain. Syb2 associated with Neuropilin 1 and Plexin A1, two essential components of the Sema3A receptor, via its juxtatransmembrane domain. Sema3A receptor and Syb2 colocalize in endosomal membranes. Moreover, upon Sema3A treatment, Syb2-deficient neurons failed to collapse and transport Plexin A1 to cell bodies. Reconstitution of Sema3A receptor in nonneuronal cells revealed that Sema3A further inhibited the exocytosis of Syb2. Therefore, Sema3A-mediated signaling and axonal repulsion require Syb2-dependent vesicular traffic.

## Introduction

The guidance of axonal and dendritic growth cones to their specific cellular target is essential for the establishment of functional neural circuits during development (Tessier-Lavigne and Goodman, 1996). Attractive and repulsive external guidance cues bind to receptors, which activates intracellular signaling pathways and reshapes the growth cone, allowing for positive and negative turning, respectively. Several types of endosomal vesicles have been identified in growth cones, but the role of exocytosis and endocytosis in growth and navigation is still largely unknown (Pfenninger, 2009). Exocytosis involves the fusion of intracellular vesicles with the plasma membrane and relies on soluble SNARE proteins located on both vesicular and plasma membranes. The synaptic vesicular SNARE Synaptobrevin 2 (Syb2; also called VAMP2) is the target of several clostridial neurotoxins, including tetanus neurotoxin (TeNT), which blocks neurotransmitter release (Schiavo et al., 2000). Knockout of Syb2 causes an almost complete loss of spontaneous and evoked release of neurotransmitters leading to postnatal death, but has not been associated with a developmental defect in the mouse brain (Schoch et al., 2001). However, there is evidence suggesting

Correspondence to Thierry Galli: thierry.galli@inserm.fr

Abbreviations used in this paper: BoNT/D, botulinum neurotoxin D; DIV, day in vitro; DRG, dorsal root ganglion; Nrp1, Neuropilin 1; PlexA1, Plexin A1; Sema, Semaphorin; SEP, Super Ecliptic Phluorin; Stx1, Syntaxin 1; Syb2, Synaptobrevin 2; Syp, Synaptophysin; TeNT, tetanus neurotoxin; TI-VAMP, tetanus insensitive–vesicle associated membrane protein.



The Rockefeller University Press $30.00
J. Cell Biol.
www.jcb.org/cgi/doi/10.1083/jcb.201106113

Published January 2, 2012

that Syb2 may play a role in the development of cultured neurons on specific substrates. Syb2 was recently shown to be required for axon formation in neurons cultured on poly-lysine but not laminin (Gupton and Gertler, 2010). TeNT inhibits calcium-triggered positive turning in neurons grown on an artificial L1 substrate but has no effect on calcium-triggered negative turning in neurons grown on laminin. The later result may suggest that exocytosis is required for attraction, but not repulsion (Tojima et al., 2007), and draw attention to Syb2 as a candidate gene for axonal guidance (Tojima et al., 2011). Previous studies using Semaphorin 3A (Sema3A) have hinted at a complex view. Indeed, repulsion mediated by Sema3A induces massive endocytosis of membrane (Fournier et al., 2000) and of its receptor (Castellani et al., 2004; Piper et al., 2005). After Sema3A-induced endocytosis of its receptor, resensitization requires reexpression and/or recycling of this receptor to the growth cone surface (Piper et al., 2005). Thus, axon guidance may depend on a regulation of both exocytosis and endocytosis.

As alluded to in the previous paragraph, it is not clear whether Syb2 functions in axonal guidance and, if so, how. Here, we took advantage of clostridial neurotoxins and genetic invalidation to demonstrate that Syb2 is required for Sema3A-mediated repulsion, but not for Sema3C-mediated attraction, in vitro and in vivo. We found that Syb2 associates with Neuropilin 1 (Nrp1) and Plexin A1 (PlexA1), two essential components of the Sema3A receptor. This interaction involves Syb2 juxtatransmembrane domain, which suggests a strong biochemical link during vesicular traffic between Syb2 and the Sema3A receptor. We further show that Sema3A inhibits the exocytosis of Syb2. Our findings thus demonstrate that Sema3A repulsion depends on Syb2-dependent vesicular traffic.

## Results and discussion

### Sema3A-mediated repulsion but not Sema3C-mediated attraction requires Syb2

To determine the function of Syb2 in axon guidance, we analyzed the guidance responses of cortical explants treated with botulinum neurotoxin D (BoNT/D; Schiavo et al., 2000) and cortical explants from Syb2 knockout mice (Schoch et al., 2001). The explants were embedded in plasma matrix facing an aggregate of cells stably secreting Sema3C, Sema3A, or mock. After 24 h of culture, we analyzed both the ratio of proximal over distal axonal length as well as the turning angles of the axons in the area perpendicular to the gradient (Fig. 1 A; Bagnard et al., 1998).

In 3D culture systems, Syb2 is not required for axonal growth of both cortical and dorsal root ganglion (DRG) neurons, as shown by BoNT/D and genetic invalidation (Fig. S1). However, we found a striking requirement of Syb2 for Sema3A-induced repulsion, but not for Sema3C-induced attraction in E15 cortical explants (Fig. 1). In the control condition, Sema3C induced an increase of axonal length in the proximal area and an attractive turning of the axons toward the source as described previously (Bagnard et al., 1998). BoNT/D treatment fully cleaved Syb2 (Fig. S1) but did not affect Sema3C-induced attraction (Fig. 1, B–E). On the contrary, Sema3A decreased axonal length in the proximal area and repelled the axons away from the source in control explants, but did not have any effect in BoNT/D-treated explants (Fig. 1, B–E). To further demonstrate the need for a functional Syb2 in Sema3A repulsion but not Sema3C attraction, we performed guidance assays in $Syb2^{+/+}$, $Syb2^{+/-}$, and $Syb2^{-/-}$ explants. We found that the absence of Syb2 in $-/-$ cortical explants abolished the repulsive effects of Sema3A, whereas it had no effect on Sema3C-mediated attraction (Fig. 1, F–I). These results demonstrate that Syb2 is required for the repulsion induced by Sema3A but not for growth or the attraction mediated by Sema3C in cortical axons ex vivo.

We then asked whether Syb2 controls the repulsive response to Sema3A by affecting the acute chemotactic responses of axonal growth cones from isolated neurons in a well-defined concentration gradient. We first cultured dissociated embryonic day 15 (E15) cortical neurons grown in microchambers framed by two reservoirs to produce a linear gradient. We then generated a Sema3A or Sema3C gradient and observed axonal growth cone turning 3 h after the onset of the gradient by time-lapse video microscopy, and quantified the results as described previously (Yam et al., 2009). We found that cortical axons respond to Sema3C by turning toward the source whether or not Syb2 was acutely inactivated by BoNT/D (Fig. 2, A and B). However, Sema3A repulsive turning was abolished by treatment with BoNT/D (Fig. 2, A and B). These experiments further show that Syb2 is not necessary for Sema3C-induced attraction, but is essential for Sema3A-induced repulsion of isolated cortical axonal growth cones.

### Sema3A-mediated repulsion requires Syb in DRG

Genetic invalidation of Sema3A induces profound defasciculation of peripheral nerves (Kitsukawa et al., 1997). However, these nerves express both Syb1 and Syb2 (Trimble et al., 1990), which, with Cellubrevin, are functionally interchangeable v-SNAREs (Deák et al., 2006; Liu et al., 2011). Thus, both Sybs1 and -2 would need to be inactivated to obliterate their function in peripheral nerves. To this end, we cultured DRG explants embedded in collagen 3D matrix facing an aggregate of cells secreting Sema3A or mock (Ben-Zvi et al., 2008), and we treated them with BoNT/D, to remove both Syb1 and Syb2. BoNT/D-treated DRG axons were not repelled by Sema3A (Fig. S2, A–C), which confirms our observations in cortical explants. Not surprisingly, in toto neurofilament immunostaining in $Syb2^{-/-}$ did not reveal a massive defasciculation of primary sensory fibers around the eyes nor in the trunk and limbs (Fig. S2 D), unlike what was observed in $Sema3A^{-/-}$ and $Nrp1^{-/-}$ mice (Kitsukawa et al., 1997). In light of the evidence of redundant function of Syb1 and Syb2 in peripheral nerves, these results suggest that the lack of guidance defect in peripheral nerves in $Syb2^{-/-}$ is likely caused by a compensatory expression of Syb1.

Published January 2, 2012

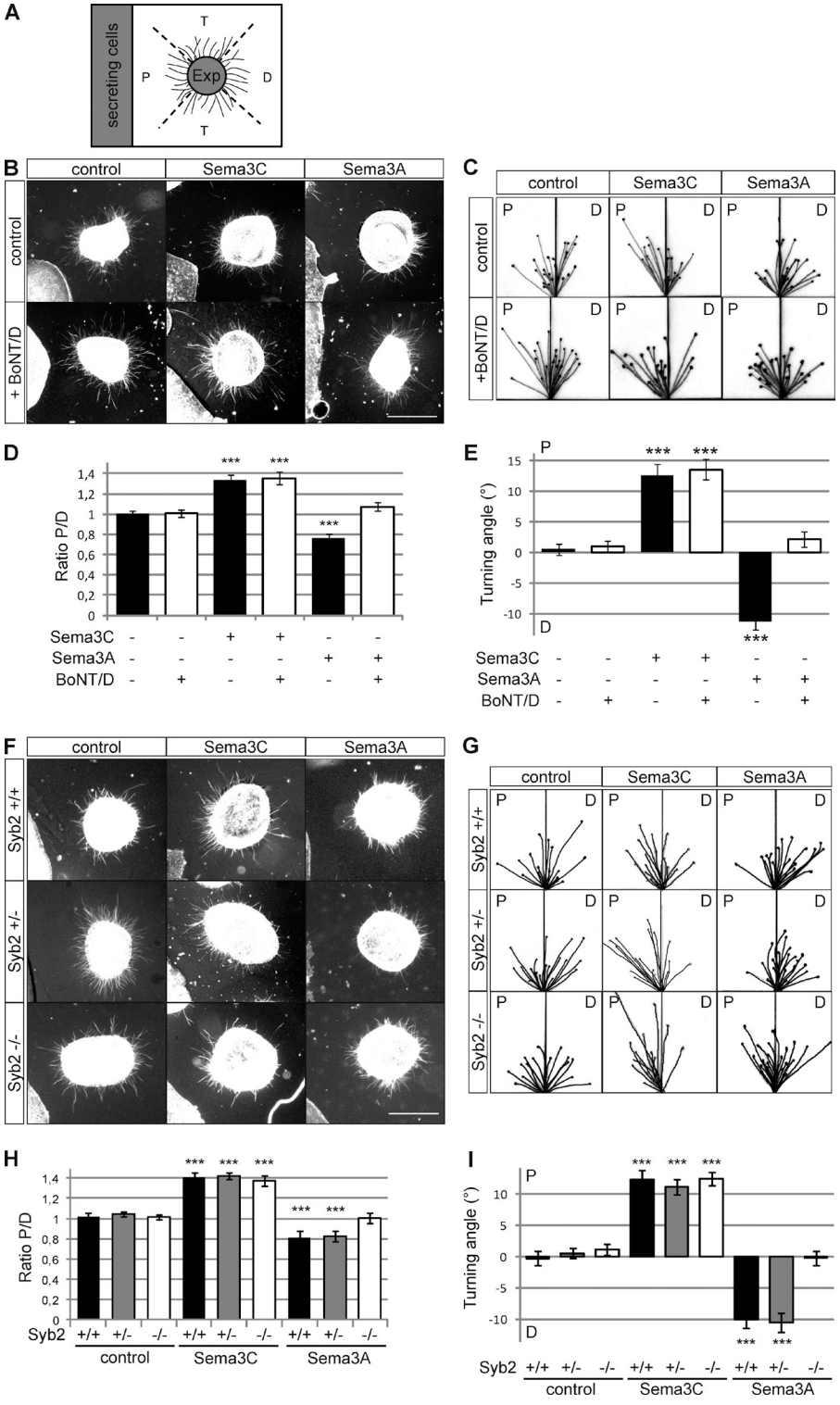


Figure 1. **Syb2 is not necessary for Sema3C-mediated attraction, but is essential for Sema3A-mediated repulsion in cortical explants.** (A) Scheme of areas quantified for each explant. P, proximal area; D, distal area; T, areas perpendicular to the gradient where turning angles were measured; Exp, cortical explant. (B) E15 cortical explants were grown in front of mock-, Sema3C-, or Sema3A-secreting cell aggregates with or without BoNT/D in the culture medium. Bar, 200 µm. (C) Axons in the areas perpendicular to the gradient were analyzed and their angles to the explants measured in different guidance conditions with or without toxin. (D) Ratio of maximal axonal lengths between proximal (P) and distal (D) areas in different guidance conditions with or without toxin (error bars indicate SEM; control, $n = 44$; control + BoNT/D, $n = 45$; Sema3C, $n = 43$; Sema3C + BoNT/D, $n = 54$; Sema3A, $n = 33$; Sema3A + BoNT/D, $n = 50$ explants). (E) Mean ± SEM values (error bars) of turning angles in the different guidance conditions with or without toxin (control, $n = 716$; control + BoNT/D, $n = 744$; Sema3C, $n = 191$; Sema3C + BoNT/D, $n = 172$; Sema3A, $n = 412$; Sema3A + BoNT/D, $n = 486$ axons). (F) E15 cortical explants from $Syb2^{+/+}$, $Syb2^{+/-}$, and $Syb2^{-/-}$ embryos were grown in front of mock-, Sema3C-, or Sema3A-secreting cell aggregates. Bar, 200 µm. (G) Axons in the areas perpendicular to the gradient were analyzed and their angles to the explants measured in the different conditions and genotypes. (H) Mean ± SEM (error bars) of the ratio of proximal over distal axonal length in different conditions and genotypes (control: $Syb2^{+/+}$, $n = 69$; $Syb2^{+/-}$, $n = 125$; $Syb2^{-/-}$, $n = 117$; Sema3C: $Syb2^{+/+}$, $n = 43$; $Syb2^{+/-}$, $n = 56$; $Syb2^{-/-}$, $n = 54$; Sema3A: $Syb2^{+/+}$, $n = 40$; $Syb2^{+/-}$, $n = 88$; $Syb2^{-/-}$, $n = 78$ explants). (I) Mean values ± SEM (error bars) of turning angles in different conditions and genotypes (control: $Syb2^{+/+}$, $n = 641$; $Syb2^{+/-}$, $n = 1{,}164$; $Syb2^{-/-}$, $n = 945$; Sema3C: $Syb2^{+/+}$, $n = 347$; $Syb2^{+/-}$, $n = 542$; $Syb2^{-/-}$, $n = 641$; Sema3A: $Syb2^{+/+}$, $n = 344$; $Syb2^{+/-}$, $n = 416$; $Syb2^{-/-}$, $n = 715$ axons). ***, $P < 0.0005$ by Student's *t* test.

## Syb2 knockout embryos display a disorganized corpus callosum

We went on to test if Syb2 inactivation would generate a defect in Sema3A-mediated guidance in the forebrain in vivo. The corpus callosum is a region where Sema3A and Sema3C play a role in axon guidance. Indeed, mutations in the Sema-binding domain of Nrp1, coreceptor of Sema3A with PlexA1 (Takahashi et al., 1999), prevent both Sema3A and Sema3C activation and generate misguidance of Nrp1-positive fibers in the corpus callosum (Hatanaka et al., 2009; Piper et al., 2009). Furthermore, a possible reduction in Nrp1-expressing axons observed in the corpus callosum of $Sema3A^{-/-}$ mice (Piper et al., 2009) may be caused by defasciculation of Nrp1-positive fibers. Thus, the lack of Sema3A repulsion in Syb2-deficient cortical neurons may generate a defect in Nrp1-positive fibers in the corpus callosum. To investigate this issue, we analyzed the

Published January 2, 2012

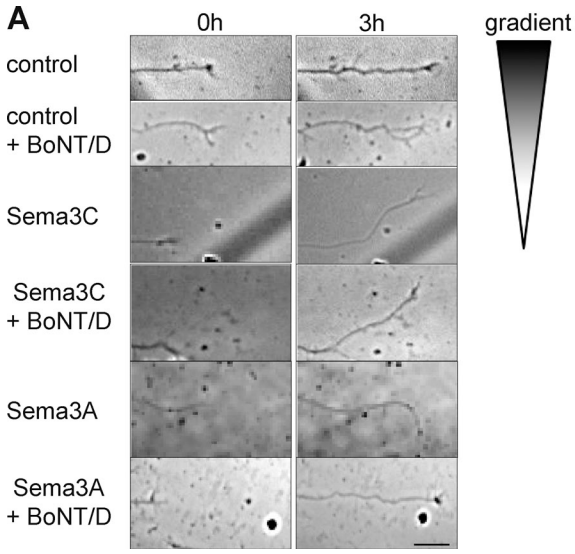


Figure 2. **Syb2 is required for Sema3A-mediated repulsion, but not Sema3C-mediated attraction, in dissociated neurons.** (A) E15 dissociated cortical neurons were grown in Ibidi microchambers in medium with or without BoNT/D. At t = 0 h, 3 µg/ml of control, Sema3C-Fc, or Sema3A-Fc medium was added at the top of the chamber. Axons were allowed to grow and turn for 3 h. Bar, 10 µm. (B) Mean values ± SEM (error bars) of axonal turning in each condition (control, *n* = 136; control + BoNT/D, *n* = 91; Sema3C, *n* = 41; Sema3C + BoNT/D, *n* = 39; Sema3A, *n* = 81; Sema3A + BoNT/D, *n* = 105 axons). **, P < 0.005 by Student's *t* test.

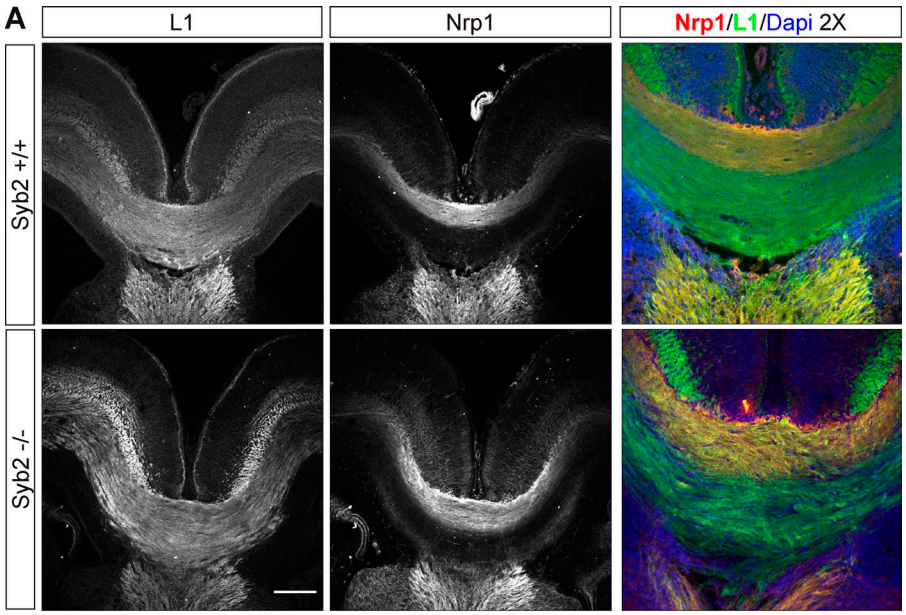


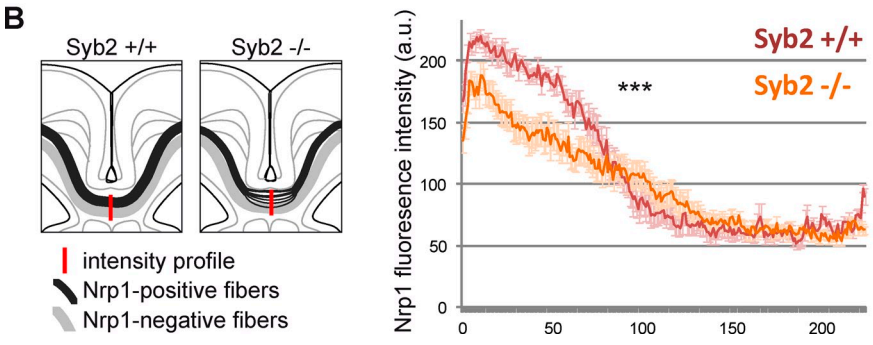


Figure 3. **Syb2$^{-/-}$ embryos display morphological defects similar to loss of Sema3A.** (A) E18 brain from Syb2$^{+/+}$ and Syb2$^{-/-}$ embryos were cut in 100-µm slices and stained with Nrp1 (red), L1 (green), and DAPI (blue; Syb2$^{+/+}$, *n* = 3; Syb2$^{-/-}$, *n* = 4 embryos). Bar, 500 µm. (B, left) Schematic view of loss of compaction of Nrp1-positive fibers in Syb2$^{-/-}$. (B, right) Profile of Nrp1 fluorescence measured in corpus callosum of Syb2$^{+/+}$ and Syb2$^{-/-}$ embryos (2–3 slices quantified for each embryo). ***, P < 0.0005 by two-way analysis of variance test.

Published January 2, 2012

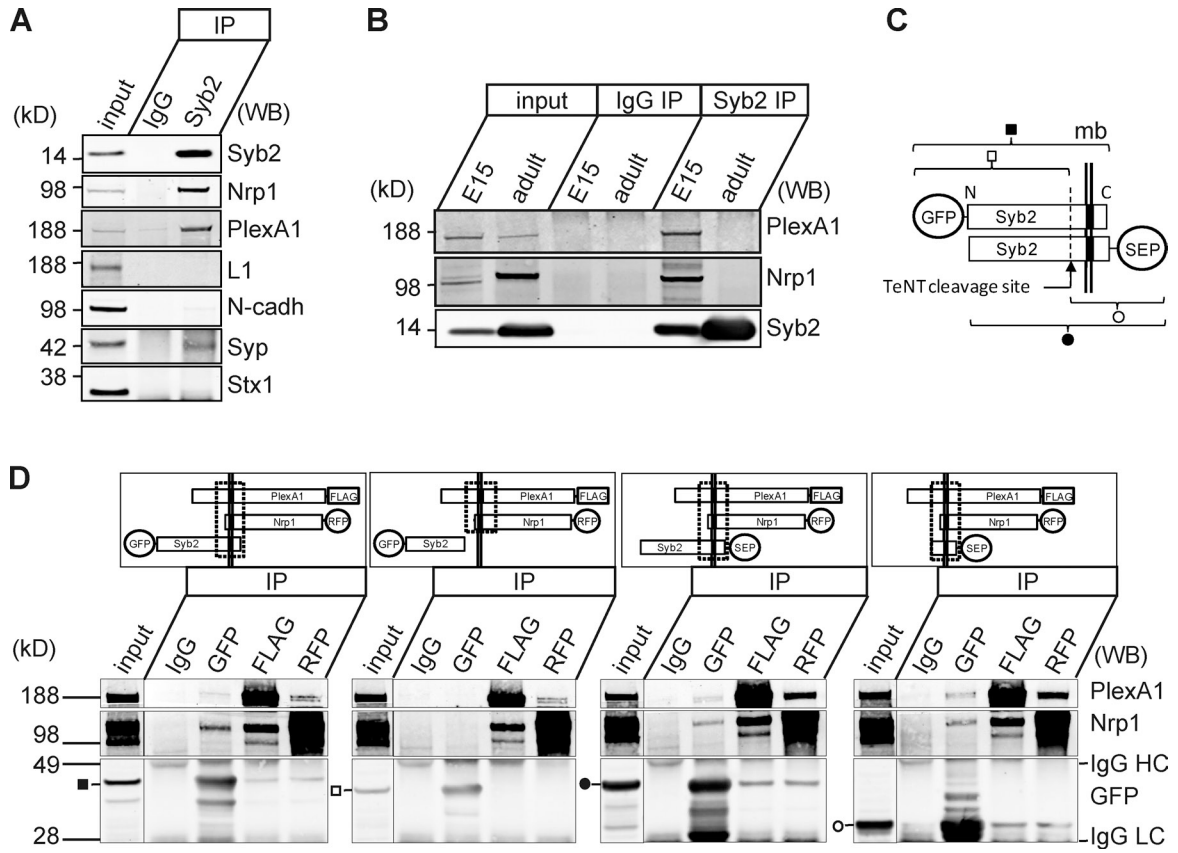


Figure 4. **Syb2 interacts with Nrp1 and PlexA1.** (A) Immunoprecipitations were performed on E15 brains using Syb2 and mouse control immunoglobulin antibodies. Coimmunoprecipitated proteins were identified by Western blotting. N-cadh, N-cadherin. (B) Syb2 and control immunoprecipitations were performed on E15 brains and adult brain. (C) Representation of GFP-Syb2 and Syb2-SEP constructs and the TeNT cleavage site. mb, membrane; closed box, GFP-Syb2 not cleaved; open box, GFP-Syb2 cleaved by TeNT; closed circle, Syb2-SEP not cleaved; open circle, Syb2-SEP cleaved by TeNT. (D) HEK-293T cells were transfected with GFP-Syb2; Syb2-SEP, Nrp1-mRFP, PlexA1-FLAG, and mutant; or wild-type TeNT plasmids. Lysates were immunoprecipitated with GFP, RFP, FLAG, and control immunoglobulin antibodies. After elution, Syb2-GFP/SEP, Nrp1-mRFP, and PlexA1-FLAG were identified by Western blotting through their respective tags. Boxes with broken lines, interacting domains. Black lines indicate that intervening lanes have been spliced out.

organization of the corpus callosum at E18 in $Syb2^{+/+}$ and $Syb2^{-/-}$ brains by immunostaining. We observed that Nrp1-positive axons presented a disorganization within the corpus callosum in $Syb2^{-/-}$ E18 embryos (Fig. 3 A), which is reminiscent of the mild phenotype described in $Sema3A^{-/-}$ mice (Piper et al., 2009), but clearly different from the one observed in $Sema3C^{-/-}$ mice (Niquille et al., 2009). Nrp1-positive fiber tract is 33% thicker in $Syb2^{-/-}$ than in $Syb2^{+/+}$ embryos (Nrp1 tract thickness as a percentage of total corpus callosum: 40.5 ± 0.97% in $Syb2^{+/+}$, 54.2 ± 1.60% in $Syb2^{-/-}$, $P = 4.18 \times 10^{-6}$ by Student's *t* test) and displayed an overall weaker staining profile in $Syb2^{-/-}$ as compared with $Syb2^{+/+}$ (Fig. 3 B). These results are in favor of a decompaction/defasciculation of Nrp1-positive fibers in the Syb2 knockout.

Altogether, these results further support the notion that Syb2 is required for Sema3A-mediated repulsion both in vitro and in vivo. We did not find any requirement for Syb2 in Sema3C-mediated attraction, which suggests the potential involvement, if any, of another traffic pathway.

### Syb2 interacts with Nrp1 and PlexA1

In vitro and in vivo studies have shown that the Sema3A receptor is composed of Nrp1 and PlexA1 (Takahashi et al., 1999). To determine the role of Syb2 in Nrp1/PlexA1 traffic, we first tested whether or not Syb2, Nrp1, and PlexA1 interact in developing neurons. We reasoned on the basis that Syb2 interacts with other vesicular proteins including Synaptophysin (Syp) and V-ATPase (Edelmann et al., 1995; Galli et al., 1996) that are sorted together into synaptic vesicles in mature neurons. Here, we found that Syb2 coimmunoprecipitated Nrp1 and PlexA1 in E15 brain extracts, but not in adult brain extracts (Fig. 4, A and B). In addition, Syb2 coimmunoprecipitated Syp, but not L1, N-cadherin, or Syntaxin 1 (Stx1), a target SNARE partner of Syb2 in neurotransmitter release, which suggests that Syb2–Nrp1–PlexA1 interaction is not a mere result of detergent solubilization (Fig. 4 A). Tetanus insensitive–vesicle associated membrane protein (TI-VAMP)/VAMP7, another v-SNARE expressed in neurons, did not coimmunoprecipitate Nrp1 and coimmunoprecipitated only small amounts of PlexA1. Furthermore, Stx1 did not coimmunoprecipitate Nrp1 or PlexA1, which provides additional evidence for the specificity of the interaction with Syb2 (Fig. S3 A). The reverse experiment using Nrp1 and PlexA1 as bait failed to coimmunoprecipitate Syb2, most likely because of the fact that the available tested antibodies could not recognize the tripartite complex because the Sema3A receptor has a specific conformation when bound to Syb2. To circumvent this problem and further identify which domain of

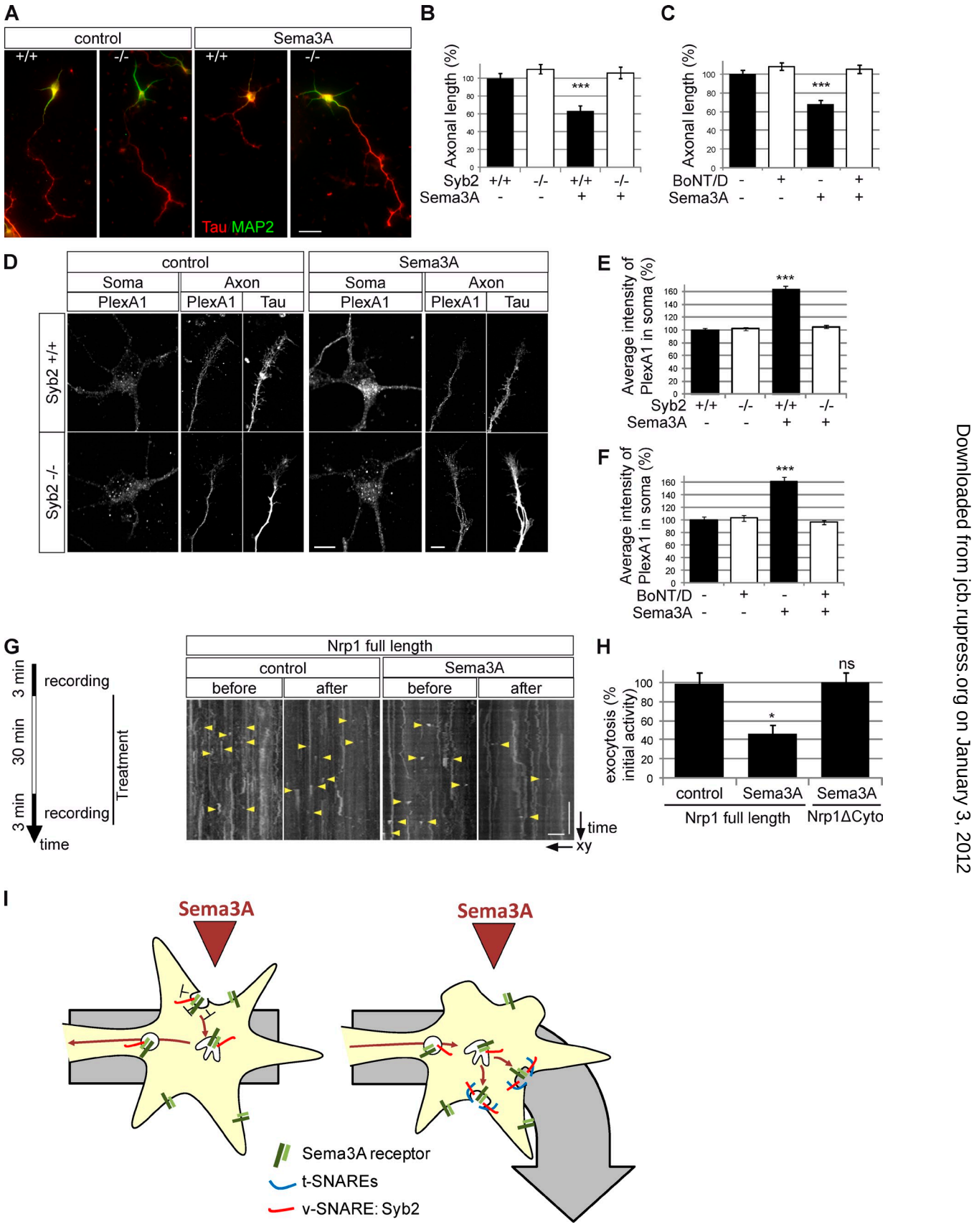


Figure 5. **Sema3A-induced repulsion requires Syb2-dependent traffic of its receptor Nrp1/PlexA1.** (A) E15 dissociated neurons from Syb2$^{+/+}$ and Syb2$^{-/-}$ embryos were grown on poly-L-lysine and laminin coverslips. At DIV2, 3 µg/ml of control or Sema3A-Fc was added to the medium. After 3 h of treatment, neurons were fixed and immunostained for MAP2 (green) and Tau (red). (B) The graph displays mean ± SEM values (error bars) of axonal

Published January 2, 2012

Syb2 mediates the interaction with Nrp1 and PlexA1, we reconstituted the complex in heterologous HEK-293T cells by expressing tagged Nrp1, PlexA1, and Syb2. GFP-Syb2, bearing GFP at the N-terminal cytosolic end, or Syb2–Super Ecliptic Phluorin (Syb2-SEP), bearing a pH-sensitive GFP at the C-terminal luminal extremity, were cleaved or not with cotransfected wild-type or mutant TeNT light chain, respectively (Fig. 4 C). The interaction between Nrp1, PlexA1, and full-length Syb2 was demonstrated by coimmunoprecipitation using each of the respective tags (Fig. 4 D). Although this interaction was maintained in the TeNT-cleaved Syb2-SEP, it was abolished in the TeNT-cleaved GFP-Syb2, showing that Syb2 interacts with Nrp1 and PlexA1 through its transmembrane and linker domain (Fig. 4 D). Additionally, Syb2 and Nrp1 strongly colocalized in intracellular membranes, particularly early endosomes (EEA1 staining) and clathrin-coated pits (AP2 labeling), when coexpressed with PlexA1 in Cos7 cells (Fig. S3 B). These results suggest that (a) the recognition between Syb2 and Nrp1/PlexA1 is highly specific, and the v-SNARE is part of a complex excluding its t-SNARE partner Stx1; and (b) Syb2 and the Sema3A receptor interact and traffic together in endocytic and/or recycling vesicles. Moreover, several single transmembrane domain proteins, including Nrp1 and Syb2, were shown to share similar structural features in their transmembrane regions susceptible to induce homo- or heterodimerization (Hubert et al., 2010). Our results showing that Syb2 interacts with Nrp1/PlexA1 through its juxtatransmembrane domain suggest that this region may play a pivotal role in sorting together Syb2, Nrp1, and PlexA1. Additional work will be required to further characterize the function of these transmembrane domains in the co-sorting of Syb2 and Sema3A receptors.

### Sema3A signaling requires Syb2 for both endocytosis and exocytosis

In developing neurons, Syb2 is transported from the Golgi apparatus to the surface of dendrites, being afterward transcytosed to the axon, where it mediates exocytosis (Sampo et al., 2003). Therefore, inactivation of Syb2 in developing neurons could lead to a defective polarization of Nrp1/PlexA1 and/or defective intracellular traffic of Nrp1/PlexA1. The first hypothesis is contradicted by the expression of Nrp1 and PlexA1 at the cell surface in Syb2$^{-/-}$ neurons (Fig. S3 C). When axons encounter an isotropic concentration of Sema3A, they collapse and retract due to massive endocytosis of the membrane and of the Nrp1/PlexA1 receptor in growth cones (Fournier et al., 2000; Piper et al., 2005). To test if Syb2 is involved in Sema3A-induced endocytosis, we measured axonal length and PlexA1 localization in dissociated cortical neurons in the presence or absence of Syb2 upon Sema3A treatment. Sema3A led to a 40% reduction of axonal length of wild-type axons, but had no effect on axonal length in the absence of Syb2 in both Syb2$^{-/-}$ or BoNT/D-treated cortical neurons (Fig. 5, A–C). Furthermore, Sema3A led to both depletion of PlexA1 in growth cones and a 60% increase of its concentration in the cell body in the presence of Syb2, but had no effect in Syb2$^{-/-}$ and BoNT/D-treated cortical neurons (Fig. 5 D–F; and Fig. S3 D). Thus, these data further demonstrate that axons lacking a functional Syb2 are insensitive to Sema3A and suggest that Syb2 is required for the endocytosis, retrograde transport of Nrp1/PlexA1 receptor upon Sema3A activation, and signaling downstream of the Sema3A receptor.

In turn, activation of the Sema3A receptor may be expected to regulate Syb2-dependent secretion. As shown earlier, Sema3A induces the collapse of growth cones, thus reducing cell surface. Decrease in growth cone cell surface complicates proper quantification of the frequency of exocytic events by optical imaging. Therefore, we reconstituted Syb2 and Sema3A receptor in a heterologous system that is not prone to collapse. We imaged Syb2-SEP exocytosis in Cos7 cells in which Nrp1 and PlexA1 were coexpressed to reconstitute Sema3A receptor. We found that control Fc treatment did not affect exocytosis, whereas the number of exocytic events decreased by 50% upon addition of Sema3A (Fig. 5, G and H; and Video 1). As a control, we found no effect of Sema3A on Syb2 exocytosis when we expressed a mutant of Nrp1 lacking its cytosolic domain (Valdembri et al., 2009). This result reveals that Sema3A signaling through Nrp1 and PlexA1 inhibits Syb2 exocytosis.

Collectively, these results suggest that Sema3A signaling requires Syb2-dependent traffic. This is in good agreement with the role of Stx1B in Sema3A repulsion (Kabayama et al., 2011). Our results further agree with the dual role of Syb2 in exocytosis and endocytosis of synaptic vesicles (Deák et al., 2004). Given that Syb2 interacts with clathrin assembly lymphoid myeloid leukemia protein (CALM), a clathrin adaptor (Koo et al., 2011), it is tempting to speculate that Syb2 is required for the endocytosis of the Sema3A receptor in growth cones. Then, as shown here, Syb2 and the Sema3A receptor would be sorted together into endosomal vesicles because of an interaction

length quantified in each condition (control: Syb2$^{+/+}$, $n$ = 47; Syb2$^{-/-}$, $n$ = 79; Sema3A: Syb2$^{+/+}$, $n$ = 30; Syb2$^{-/-}$, $n$ = 59 axons). Bar, 10 µm. (C) Mean values ± SEM (error bars) of axonal length quantified in each condition (control, $n$ = 88; control + BoNT/D, $n$ = 101; 3 µg/ml Sema3A, $n$ = 97; 3 µg/ml Sema3A + BoNT/D, $n$ = 99 axons). ***, P < 0.0005 by Student's $t$ test. (D) Immunofluorescence of PlexA1 and Tau in dissociated cortical neurons cultured from Syb2$^{-/-}$ or Syb2$^{+/+}$ embryos and treated for 30 min with or without 1 µg/ml Sema3A. Bar, 2 µm. (E) Mean intensity of PlexA1 in soma of cortical neurons (control: Syb2$^{+/+}$, $n$ = 129; Syb2$^{-/-}$, $n$ = 109; Sema3A: Syb2$^{+/+}$, $n$ = 129; Syb2$^{-/-}$, $n$ = 162 somas in two embryos per genotype). (F) Mean intensity of PlexA1 in soma of cortical neurons (control, $n$ = 41; control + BoNT/D, $n$ = 50; Sema3A, $n$ = 64; Sema3A + BoNT/D, $n$ = 55 somas). (G) Scheme of Syb2-SEP exocytosis protocol. Cos7 cells were cotransfected with PlexA1-FLAG, Syb2-SEP, and Nrp1-mRFP full length or Nrp1ΔCyto-mRFP, and exocytic events of Syb2-SEP were recorded for 3 min. After 30 min of treatment with control (Fc) or Sema3A (Sema3A-Fc), the same cell was recorded for an additional 3 min. Kymographs of recorded cells before and after treatment are shown; exocytic events appear as bright spots, marked with arrowheads. (H) Quantification of Syb2-SEP exocytic events. To evaluate the effect of treatment, exocytic events in the second recording are expressed as a percentage of the first recording for each cell (Nrp1 full length in control, $n$ = 4; and Sema3A condition, $n$ = 8 cells; Nrp1ΔCyto in Sema3A condition, $n$ = 8 cells). Vertical bar, 10 s; horizontal bar, 10 µm. Error bars indicate SEM. (I) Proposed model: Sema3A induces a local disequilibrium (endocytosis → exocytosis) in the growth cone, generating a local surface shrinkage, and prevents progression of the growth cone in the direction of the source, favoring turning to the opposite direction. Syb2 interacts with Nrp1 and PlexA1 and is required for their traffic.

Published January 2, 2012

mediated by their transmembrane domains. Sema3A further inhibited Syb2-dependent exocytosis when we reconstituted Sema3A receptor in nonneuronal cells. On this basis, we consider that the model proposing that attraction relies on Syb2 exocytosis, whereas repulsion relies on endocytosis (Tojima et al., 2011), needs to be revised. We instead propose that the molecular mechanism of Sema3A repulsion is based on fine tuning of the opposing processes of Syb2-dependent endocytosis and exocytosis (Fig. 5 I). Sema3A would induce a local disequilibrium at the site facing the Sema3A source by simultaneously triggering endocytosis and inhibiting exocytosis. Such a combination of locally increased endocytosis and decreased exocytosis would prevent progression in the direction of the source, favor turning of the growth cone in the opposite direction, and resensitize it to Sema3A (Piper et al., 2005). It is possible that TI-VAMP's role in Netrin1 attraction (Cotrufo et al., 2011) may also be based on a change of exocytosis/endocytosis equilibrium, further generalizing the principle unraveled here. Therefore we propose that a main function of Syb2 in developing neurons is to traffic Sema3A receptor, allowing for its endocytosis, traffic away from the Sema3A source, and reexpression at the cell surface by exocytosis. It now remains to be tested whether the primary role of Syb2 resides in endocytosis or exocytosis of the Sema3A receptor, and how Sema3A signaling controls Syb2 exocytosis.

## Materials and methods

### Antibodies

The following antibodies were used: Nrp1 (Western blotting [WB], 1/1,000 [Millipore]; immunofluorescence [IF], 1/500; [R&D Systems]), PlexA1 (WB, 1/1,000; IF, 1/500; Abcam), tubulin (IF, 1/10,000; Developmental Studies Hybridoma Bank), AP2 (WB, 1/1,000 [Abcam]; IF, 1/1,000; Thermo Fisher Scientific), L1 (a gift from F. Rathjen, Max-Delbrück-Centrum für Molekulare Medizin, Berlin, Germany; WB, 1/1,000; IF, 1/200), Syb2 (69.1 clone, a gift from R. Jahn, Max Planck Institute, Göttingen, Germany; WB, 1/10,000; IF, 1/1,000), Syntaxin1 (HPC1 clone, a gift from C. Barnstable, Yale University, New Haven, CT; WB, 1/10,000), Syp (7.2 clone, a gift from R. Jahn, Max Planck Institute, Goettingen, Germany; WB, 1/500), control IgG (Sigma-Aldrich), TI-VAMP (158.2; WB, 1/1,000), Tau (Millipore; IF, 1/1,000), EEA1 (Applied Biosystems; IF, 1/500), FLAG (Sigma Aldrich), GFP (Roche) and RFP (Millipore). DAPI was from Invitrogen.

### Guidance assays

**Explant assays.** We are grateful to T. Südhof (Stanford University, Stanford, CA) for the generous gift of the Syb2 knockout mouse. E13 and E15 embryos were extracted from Syb2 strain or Swiss mice, and DRG and cortical explants were embedded in front of stably transfected Sema3A, Sema3C, or mock-secreting cells, in 3D matrices, as described previously (Bagnard et al., 1998; Ben-Zvi et al., 2008). In brief, DRG and cortex were extracted in cold D-PBS and GBSS + glucose, respectively. DRGs were placed on a cushion of collagen gel in front of an aggregate of mock or Sema3A-secreting cells before the application of a second cushion of collagen containing 100 ng/ml h-NGF (Euromedex). Blocks of cortex (~200 µm in diameter) were positioned next to an aggregate of mock-, Sema3A-, or Sema3C-secreting cells in 20 µl of chicken plasma supplemented with 0.8 U thrombin (Sigma-Aldrich). Neuronal culture medium (Neurobasal 1×, 2% B27, 1% L-glutamine, and 1% penicillin/streptomycin) was added after polymerization of the matrices. Cultures were fixed after 24 h of culture and immunostained for tubulin to analyze axonal lengths and surfaces as described previously (Bagnard et al., 1998).

**Microchamber assays.** E15 cortical neurons from the SWISS strain were dissected and dissociated before being plated at 10 µl of $6 \times 10^6$ cells/ml in loaded medium (MEM 1×, 10% SVF, 1% L-glutamine, and 1% penicillin/streptomycin) in the observation area of hydrophobic chambers (Ibidi) precoated with poly-L-lysine and laminin (10 µg/ml each). Neurons were allowed to attach overnight before loading the neuronal culture medium with or without 30 nM BoNT/D. At day in vitro 2 (DIV2), 3 µg/ml of guidance cues were added or not added in the top chamber, and neurons were imaged for 3 h. Turning angles were measured as described previously (Yam et al., 2009).

**Collapse assays.** E15 cortical neurons from Syb2 or SWISS strains were dissected and dissociated before being plated in loaded medium, on glass coverslips precoated with poly-L-lysine and laminin (10 µg/ml each, overnight in D-PBS and 3 h in Neurobasal medium, respectively). After 3 h of attachment, culture medium was changed to neuronal medium with or without 30 nM BoNT/D. At DIV2, 1 or 3 µg/ml Sema3A-Fc or plain media was added on cortical culture in fresh neuronal medium and incubated for 3 h before fixation with 4% paraformaldehyde (PFA)–4% sucrose and immunostaining.

### Immunoprecipitation

We are grateful to V. Castellani (Université Claude Bernard Lyon, Villeurbanne, France) for PlexinA1-FLAG cDNA. E15 brain or DIV1 transfected HEK-293T cells were lysed in lysis buffer (TSE-1% Triton X-100, 1% Complete [Roche]) at 4°C. After 20 min of centrifugation at 13,000 *g*, total proteins were quantified with Bradford assays. 1 mg of total proteins was incubated overnight at 4°C with 5 µg of antibody and 150 µg of protein G Dynabeads (Applied Biosystems), prewashed with lysis buffer. After removal of supernatant and three washes of beads with lysis buffer, proteins were eluted in SDS buffer (loading buffers were obtained from Applied Biosystems) and incubated for 10 min at 95°C. Eluted proteins were finally loaded on 4–12% BisTris NuPAGE gel (Applied Biosystems). The gel was run and transferred to nitrocellulose membrane for Western blot staining. The membrane was blocked by incubation with TBS-1% Tween-20, 5% milk before incubation of primary antibody in TBS-1% Tween-20, 5% milk. After three washes, fluorescent secondary antibodies TBS-1% Tween-20 were incubated, and protein staining was revealed with the Odyssey system (LI-COR Biosciences).

### Immunostaining

**In vitro immunofluorescence.** DIV2 E15 neurons or Cos7 cell cultures were fixed for 20 min with 4% PFA; quenched for 20 min in PBS 1× and 50 mM $NH_4Cl$; permeabilized 4 min in PBS 1× and 0.1% Triton X-100; and blocked for 30 min in PBS 1× and 2.5% fish gelatin. Primary antibodies were incubated either overnight at 4°C or for 2 h at room temperature, in PBS 1× and 0.125% fish gelatin. After washes, secondary antibodies were incubated for 45 min at room temperature before mounting in Prolong medium (Applied Biosystems). For surface staining, DIV2 E15 neurons were processed as described previously without the permeabilization step.

**In vivo immunofluorescence.** E18 brains were fixed overnight in 4% PFA, washed in PBS 1×, and embedded in 3% low-melt agarose for vibratome sectioning. Slices were first permeabilized for 3 h in PBS 1×, 1% Triton X-100, and 0.25% fish gelatin before incubation of primary antibodies for 2 d at 4°C in PBS 1×, 0.1% Triton X-100, and 0.125% fish gelatin. Slices were washed three times for 2 h, then secondary antibodies were incubated overnight at 4°C before mounting of slices in Vectashield medium (Vector Laboratories).

**In toto immunofluorescence.** E12 embryos were fixed overnight in 4% PFA; washed in PBS 1×; dried in methanol series before being whitened 3 h in 80% methanol, 5% DMSO, and 1% $H_2O_2$ (Huber et al., 2005); and permeabilized for 3 h in PBS 1×, 1% Triton X-100, and 5% milk. Embryos were incubated with 1/100 2H3 primary antibodies in PBS 1× and 1% Triton X-100 for 2 d at room temperature, washed three times for 3 h, and incubated with Cy3-goat anti–mouse secondary antibodies and DAPI for 1 d at room temperature.

### Transfection

Cos7 cells were transfected with an Amaxa system according to the manufacturer's instructions (Lonza). HEK-293T cells were transfected with Lipofectamine 2000 (Invitrogen) according to the manufacturer's instructions.

### Time-lapse video microscopy

Syb2-SEP time-lapse video imaging was performed in modified Krebs-Ringer-Hepes buffer (140 mM NaCl, 4.7 mM KCl, 2 mM $MgCl_2$, 1 mM $CaCl_2$, 10 mM Hepes, and 5.5 mM glucose, pH 7.4) at 37°C with an inverted epifluorescence microscope (DMI6000B; Leica) modified to use laser illumination. The 488-nm argon ion laser beam was sufficiently expanded to get near uniform illumination. Fluorescent excitation and collection were performed with 63×/1.6 NA Plan-Apochromat oil-immersion objective lenses. Images were acquired every 500 ms, with an integration

time of 100 ms using a highly sensitive EM charge-coupled device camera (Cascade 512B; Roper Scientific) controlled by MetaMorph software (Molecular Devices).

**Fluorescent microscopy**

For explants assays, images were taken with a 2.5× objective lens on microscope (DMRD; Leica) controlled by MetaVue software (Molecular Devices). In vitro and in vivo immunofluorescence images were taken with, respectively, oil-immersion 40× or 63× and dry 10× or 20× objective lenses in a confocal microscope (TCS SP5; Leica) controlled the Leica Application Suite. In toto embryo images were taken with a 0.8× dry objective lens in a stereomicroscope (LUMAR; Carl Zeiss) and assembled with CombineZ software. Axon lengths and surfaces were analyzed using MetaMorph software (Molecular Devices). Axon turnings quantifications were performed with ImageJ.

**Online supplemental material**

Fig. S1 demonstrates that Syb2 is not involved in axonal growth in both E15 cortical and E13 DRG neurons. Fig. S2 shows that Syb2 is necessary for Sema3A-mediated repulsion but not Sema3A-induced growth inhibition in E13 DRG; E12 Syb2 knockout embryos do not display major defect in peripheral nerves, likely because of compensation by Syb1. Fig. S3 shows control immunoprecipitation experiments (Tl-VAMP and Syntaxin1 as baits) in E15 brain; the colocalization of Syb2, Nrp1, and endocytic markers; the surface labeling of Nrp1 and PlexA1 in Syb2 knockout E15 cortical neurons; and labeling related to the graph in Fig. 5 F. Video 1 displays the effect of Sema3A on Syb2-exocytosis imaged with Syb2-SEP in a Cos7 cell. Online supplemental material is available at http://www.jcb.org/cgi/content/full/jcb.201106113/DC1.

We are grateful to Lydia Danglot, Alessandra Pierani, Marie-Christine Simmler, and David Tareste, for critical reading of the manuscript. We are grateful to Alessandra Pierani, Patricia Gaspar, and the Galli laboratory for helpful discussions.

Work in our group was funded in part by grants from Institut National de la Santé et de la Recherche Médicale, the Association Française contre les Myopathies (AFM), the Association pour la Recherche sur le Cancer (ARC), the Mairie de Paris Medical Research and Health Program, the Fondation pour la Recherche Médicale (FRM), the Ecole des Neurosciences de Paris (ENP; to T. Galli). K. Zylbersztejn was supported by a Bourse de Docteur Ingénieur (BDI) fellowship from the Centre National de la Recherche Scientifique and a doctoral fellowship from the FRM. M. Petkovic was supported by the ENP PhD program. A. Burgo was supported by FRM and Mairie de Paris. G. Serini was supported by Telethon and Associazione Italiana per la Ricerca sul Cancro (AIRC). M. Deck was supported by the ARC, and S. Garel was supported by a starting grant from the City of Paris and the European Young Investigators program.

Author contributions: K. Zylbersztejn and T. Galli conceived and designed the experiments, analyzed data, and wrote the paper. K. Zylbersztejn, M. Petkovic, A. Burgo, and M. Deck performed experiments. S. Garel, S. Marcos, E. Bloch-Gallego, F. Nothias, D. Bagnard, T. Binz, and G. Serini helped to set up the project, provided reagents, and co-wrote the paper.

Submitted: 20 June 2011
Accepted: 1 December 2011

## References

Bagnard, D., M. Lohrum, D. Uziel, A.W. Püschel, and J. Bolz. 1998. Semaphorins act as attractive and repulsive guidance signals during the development of cortical projections. *Development*. 125:5043–5053.

Ben-Zvi, A., L. Ben-Gigi, Z. Yagil, O. Lerman, and O. Behar. 2008. Semaphorin3A regulates axon growth independently of growth cone repulsion via modulation of TrkA signaling. *Cell. Signal.* 20:467–479. http://dx.doi.org/10.1016/j.cellsig.2007.10.023

Castellani, V., J. Falk, and G. Rougon. 2004. Semaphorin3A-induced receptor endocytosis during axon guidance responses is mediated by L1 CAM. *Mol. Cell. Neurosci.* 26:89–100. http://dx.doi.org/10.1016/j.mcn.2004.01.010

Cotrufo, T., F. Pérez-Brangulí, A. Muhaisen, O. Ros, R. Andrés, T. Baeriswyl, G. Fuschini, T. Tarrago, M. Pascual, J. Ureña, et al. 2011. A signaling mechanism coupling netrin-1/deleted in colorectal cancer chemoattraction to SNARE-mediated exocytosis in axonal growth cones. *J. Neurosci.* 31:14463–14480. http://dx.doi.org/10.1523/JNEUROSCI.3018-11.2011

Deák, F., S. Schoch, X. Liu, T.C. Südhof, and E.T. Kavalali. 2004. Synaptobrevin is essential for fast synaptic-vesicle endocytosis. *Nat. Cell Biol.* 6:1102–1108. http://dx.doi.org/10.1038/ncb1185

Deák, F., O.H. Shin, E.T. Kavalali, and T.C. Südhof. 2006. Structural determinants of synaptobrevin 2 function in synaptic vesicle fusion. *J. Neurosci.* 26:6668–6676. http://dx.doi.org/10.1523/JNEUROSCI.5272-05.2006

Edelmann, L., P.I. Hanson, E.R. Chapman, and R. Jahn. 1995. Synaptobrevin binding to synaptophysin: a potential mechanism for controlling the exocytotic fusion machine. *EMBO J.* 14:224–231.

Fournier, A.E., F. Nakamura, S. Kawamoto, Y. Goshima, R.G. Kalb, and S.M. Strittmatter. 2000. Semaphorin3A enhances endocytosis at sites of receptor-F-actin colocalization during growth cone collapse. *J. Cell Biol.* 149:411–422. http://dx.doi.org/10.1083/jcb.149.2.411

Galli, T., P.S. McPherson, and P. De Camilli. 1996. The V0 sector of the V-ATPase, synaptobrevin, and synaptophysin are associated on synaptic vesicles in a Triton X-100-resistant, freeze-thawing sensitive, complex. *J. Biol. Chem.* 271:2193–2198. http://dx.doi.org/ 10.1074/jbc.271.4.2193

Gupton, S.L., and F.B. Gertler. 2010. Integrin signaling switches the cytoskeletal and exocytic machinery that drives neuritogenesis. *Dev. Cell*. 18:725–736. http://dx.doi.org/10.1016/j.devcel.2010.02.017

Hatanaka, Y., T. Matsumoto, Y. Yanagawa, H. Fujisawa, F. Murakami, and M. Masu. 2009. Distinct roles of neuropilin 1 signaling for radial and tangential extension of callosal axons. *J. Comp. Neurol.* 514:215–225. http://dx.doi.org/10.1002/cne.22021

Huber, A.B., A. Kania, T.S. Tran, C. Gu, N. De Marco Garcia, I. Lieberam, D. Johnson, T.M. Jessell, D.D. Ginty, and A.L. Kolodkin. 2005. Distinct roles for secreted semaphorin signaling in spinal motor axon guidance. *Neuron*. 48:949–964. http://dx.doi.org/10.1016/j.neuron.2005.12.003

Hubert, P., P. Sawma, J.P. Duneau, J. Khao, J. Hénin, D. Bagnard, and J. Sturgis. 2010. Single-spanning transmembrane domains in cell growth and cell-cell interactions: More than meets the eye? *Cell Adh Migr*. 4:313–324. http://dx.doi.org/10.4161/cam.4.2.12430

Kabayama, H., M. Takeuchi, M. Taniguchi, N. Tokushige, S. Kozaki, A. Mizutani, T. Nakamura, and K. Mikoshiba. 2011. Syntaxin 1B suppresses macropinocytosis and semaphorin 3A-induced growth cone collapse. *J. Neurosci.* 31:7357–7364. http://dx.doi.org/10.1523/JNEUROSCI.2718-10.2011

Kitsukawa, T., M. Shimizu, M. Sanbo, T. Hirata, M. Taniguchi, Y. Bekku, T. Yagi, and H. Fujisawa. 1997. Neuropilin-semaphorin III/D-mediated chemorepulsive signals play a crucial role in peripheral nerve projection in mice. *Neuron*. 19:995–1005. http://dx.doi.org/10.1016/S0896-6273(00)80392-X

Koo, S.J., S. Markovic, D. Puchkov, C.C. Mahrenholz, F. Beceren-Braun, T. Maritzen, J. Dernedde, R. Volkmer, H. Oschkinat, and V. Haucke. 2011. SNARE motif-mediated sorting of synaptobrevin by the endocytic adaptors clathrin assembly lymphoid myeloid leukemia (CALM) and AP180 at synapses. *Proc. Natl. Acad. Sci. USA*. 108:13540–13545. http://dx.doi.org/10.1073/pnas.1107067108

Liu, Y., Y. Sugiura, and W. Lin. 2011. The role of synaptobrevin1/VAMP1 in Ca2+-triggered neurotransmitter release at the mouse neuromuscular junction. *J. Physiol.* 589:1603–1618. http://dx.doi.org/10.1113/jphysiol.2010.201939

Niquille, M., S. Garel, F. Mann, J.P. Hornung, B. Otsmane, S. Chevalley, C. Parras, F. Guillemot, P. Gaspar, Y. Yanagawa, and C. Lebrand. 2009. Transient neuronal populations are required to guide callosal axons: a role for semaphorin 3C. *PLoS Biol.* 7:e1000230. http://dx.doi.org/10.1371/journal.pbio.1000230

Pfenninger, K.H. 2009. Plasma membrane expansion: a neuron's Herculean task. *Nat. Rev. Neurosci.* 10:251–261. http://dx.doi.org/10.1038/nrn2593

Piper, M., S. Salih, C. Weinl, C.E. Holt, and W.A. Harris. 2005. Endocytosis-dependent desensitization and protein synthesis-dependent resensitization in retinal growth cone adaptation. *Nat. Neurosci.* 8:179–186. http://dx.doi.org/10.1038/nn1380

Piper, M., C. Plachez, O. Zalucki, T. Fothergill, G. Goudreau, R. Erzurumlu, C. Gu, and L.J. Richards. 2009. Neuropilin 1-Sema signaling regulates crossing of cingulate pioneering axons during development of the corpus callosum. *Cereb. Cortex*. 19:i11–i21. http://dx.doi.org/10.1093/cercor/bhp027

Sampo, B., S. Kaech, S. Kunz, and G. Banker. 2003. Two distinct mechanisms target membrane proteins to the axonal surface. *Neuron*. 37:611–624. http://dx.doi.org/10.1016/S0896-6273(03)00058-8

Schiavo, G., M. Matteoli, and C. Montecucco. 2000. Neurotoxins affecting neuroexocytosis. *Physiol. Rev.* 80:717–766.

Schoch, S., F. Deák, A. Königstorfer, M. Mozhayeva, Y. Sara, T.C. Südhof, and E.T. Kavalali. 2001. SNARE function analyzed in synaptobrevin/VAMP knockout mice. *Science*. 294:1117–1122. http://dx.doi.org/10.1126/science.1064335

Takahashi, T., A. Fournier, F. Nakamura, L.H. Wang, Y. Murakami, R.G. Kalb, H. Fujisawa, and S.M. Strittmatter. 1999. Plexin-neuropilin-1 complexes

form functional semaphorin-3A receptors. *Cell*. 99:59–69. http://dx.doi.org/10.1016/S0092-8674(00)80062-8

Tessier-Lavigne, M., and C.S. Goodman. 1996. The molecular biology of axon guidance. *Science*. 274:1123–1133. http://dx.doi.org/10.1126/science.274.5290.1123

Tojima, T., H. Akiyama, R. Itofusa, Y. Li, H. Katayama, A. Miyawaki, and H. Kamiguchi. 2007. Attractive axon guidance involves asymmetric membrane transport and exocytosis in the growth cone. *Nat. Neurosci.* 10:58–66. http://dx.doi.org/10.1038/nn1814

Tojima, T., J.H. Hines, J.R. Henley, and H. Kamiguchi. 2011. Second messengers and membrane trafficking direct and organize growth cone steering. *Nat. Rev. Neurosci.* 12:191–203. http://dx.doi.org/10.1038/nrn2996

Trimble, W.S., T.S. Gray, L.A. Elferink, M.C. Wilson, and R.H. Scheller. 1990. Distinct patterns of expression of two VAMP genes within the rat brain. *J. Neurosci.* 10:1380–1387.

Valdembri, D., P.T. Caswell, K.I. Anderson, J.P. Schwarz, I. König, E. Astanina, F. Caccavari, J.C. Norman, M.J. Humphries, F. Bussolino, and G. Serini. 2009. Neuropilin-1/GIPC1 signaling regulates alpha5beta1 integrin traffic and function in endothelial cells. *PLoS Biol.* 7:e25. http://dx.doi.org/10.1371/journal.pbio.1000025

Yam, P.T., S.D. Langlois, S. Morin, and F. Charron. 2009. Sonic hedgehog guides axons through a noncanonical, Src-family-kinase-dependent signaling pathway. *Neuron*. 62:349–362. http://dx.doi.org/10.1016/j.neuron.2009.03.022

Published January 2, 2012



Zylbersztejn et al., http://www.jcb.org/cgi/content/full/jcb.201106113/DC1

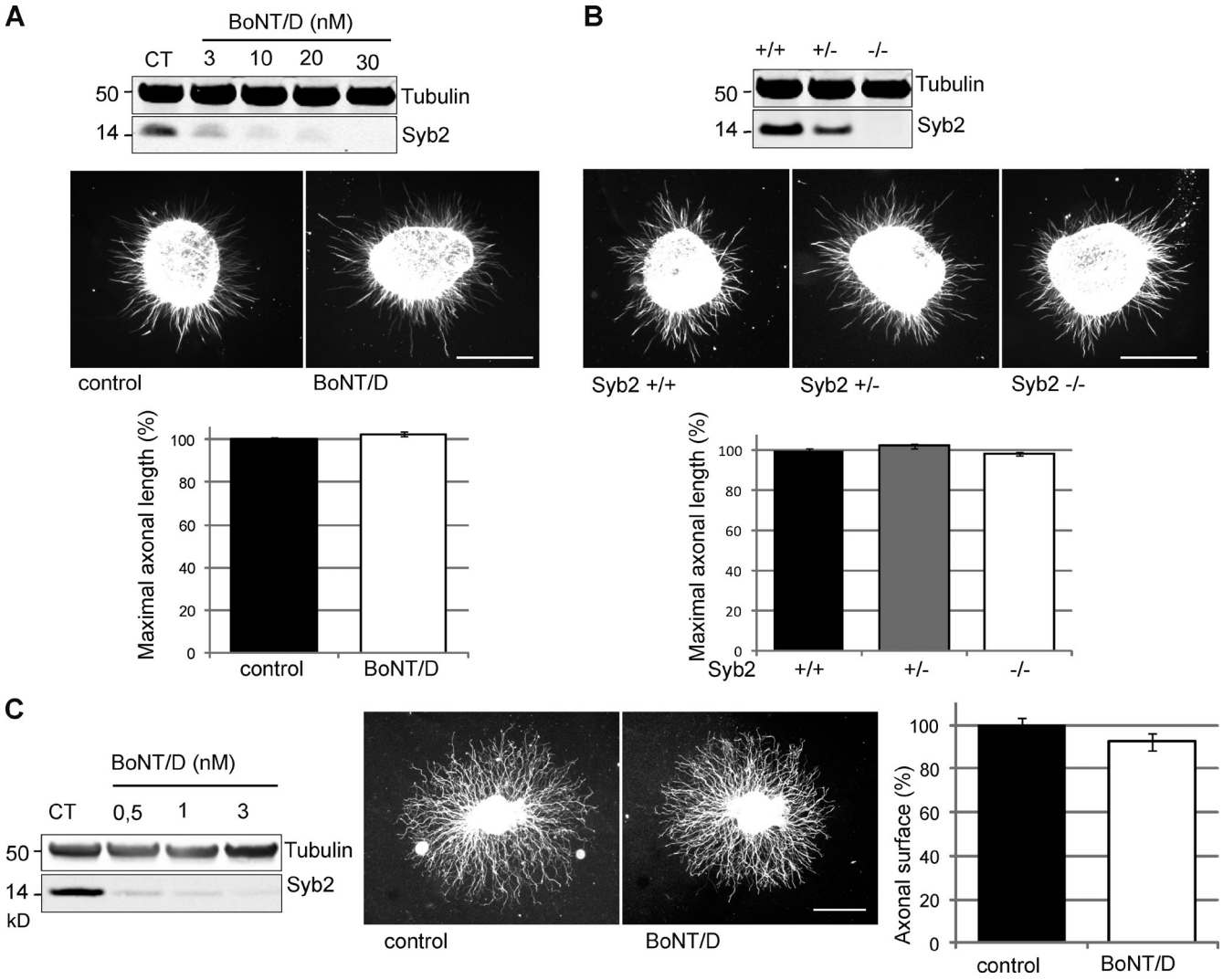


Figure S1. **Inactivation of Syb2 in E15 cortical or E13 DRG explants does not affect axonal growth.** (A, top) E15 cortical explants were grown on poly-L-lysine and laminin-coated dishes with increasing concentrations of BoNT/D in the medium. After 15 h of treatment, tubulin and Syb2 were detected by Western blotting in cell lysates. (A, middle) Representative images of E15 cortical explants grown in plasma matrix for 24 h with or without 30 nM BoNT/D in the medium. (A, bottom) The quantification of maximal axonal length displayed as mean ± SEM values (error bars) for each condition (control, $n = 89$; BoNT/D, $n = 85$ explants). (B, top) E15 cortex from Syb2$^{+/+}$, Syb2$^{+/-}$, and Syb2$^{-/-}$ embryos were analyzed by Western blotting to demonstrate the complete loss of Syb2 in Syb2$^{-/-}$ embryos. (B, middle) Representative images of E15 cortical explants from Syb2$^{+/+}$, Syb2$^{+/-}$, and Syb2$^{-/-}$ embryos grown in plasma matrix. (B, bottom) The quantification of maximal axonal length displayed as mean ± SEM values (error bars) for each genotype (Syb2$^{+/+}$, $n = 100$; Syb2$^{+/-}$, $n = 121$; Syb2$^{-/-}$, $n = 174$ explants). (C, left) Western blot analysis of Tubulin and Syb2 after cleavage of Syb2 with increasing concentrations of BoNT/D in the DRG explants. (C, middle) Representative images of DRGs grown in collagen gel with or without 3 nM BoNT/D toxin added to the culture medium. (C, right) Quantification of total axonal surface of DRG explants in control or 3 nM BoNT/D condition expressed as means ± SEM (error bars; control, $n = 48$; BoNT/D, $n = 57$ explants). Bars, 200 µm.

Published January 2, 2012

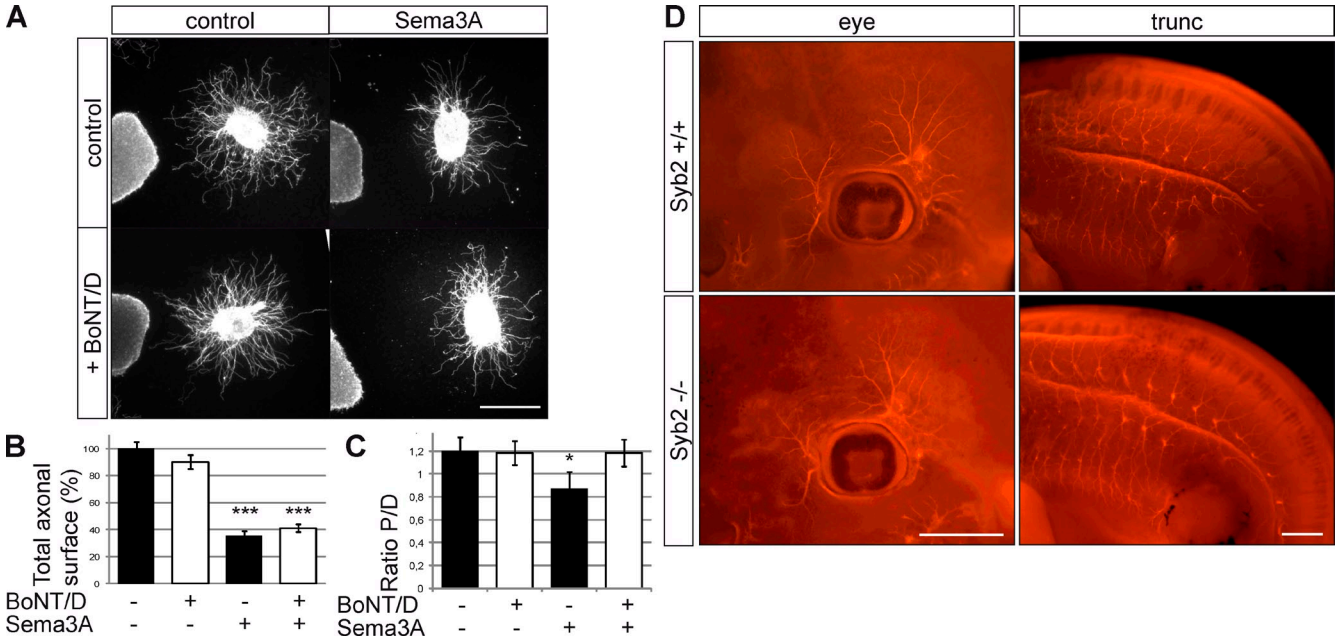


Figure S2. **Lack of peripheral nervous system defect in Syb2$^{-/-}$ embryos.** (A) E13 DRG explants were grown in matrix supplemented with 100 ng/ml NGF in front of mock- or Sema3A-secreting cell aggregates with or without BoNT/D in the medium. Bar, 200 µm. (B and C) In each condition, total axonal surface and the ratio of proximal over distal axonal areas was quantified (error bars indicate means ± SEM; control, $n = 13$; control + BoNT/D, $n = 13$; Sema3A, $n = 16$; Sema3A + BoNT/D, $n = 18$ explants). Note that repulsion, but not growth, was inhibited by BoNT/D. Previous studies have revealed that Sema3A also competes with NGF for binding to TrkA and inhibits axonal outgrowth of DRG neurons. This result suggests that Syb1/2 are involved in Sema3A-mediated guidance, which is dependent on Nrp1/PlexA1but not in Sema3A-induced TrkA-dependent axonal growth inhibition. *, $P < 0.05$; ***, $P < 0.0005$ by Student's *t* test. (D) E12 Syb2$^{+/+}$ and Syb2$^{-/-}$ embryos were stained in toto with neurofilament 2H3 antibody ($n = 3$ embryos each). Bars, 500 µm.

Published January 2, 2012

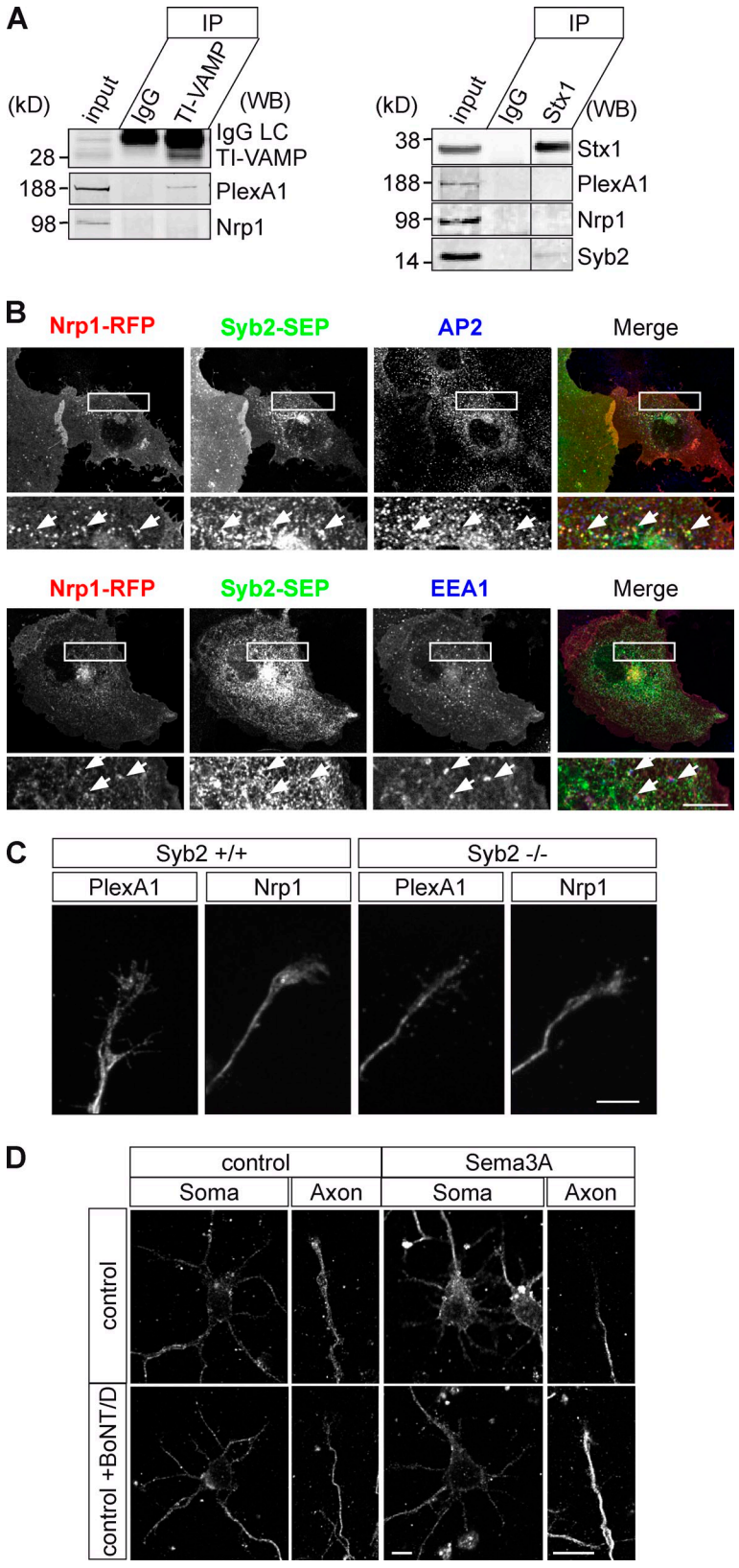


Figure S3. **Colocalization of Syb2 and Sema3A receptor in endocytic membranes.** (A) Tl-VAMP, Stx1, and control immunoglobulin immunoprecipitations were performed on E15 brains. Coimmunoprecipitated proteins were identified by Western blotting. Black lines indicate that intervening lanes have been spliced out. (B) Immunofluorescence in Cos7 cells of exogenous Nrp1-mRFP and Syb2-SEP with AP2 or EEA1. Colocalizations are marked with arrows. Bottom panels show enlarged views of the boxed regions. Bar, 10 µm. (C) Surface staining of PlexA1 and Nrp1 in $Syb2^{+/+}$ and $Syb2^{-/-}$ DIV2 E15 cortical neurons. (D) Immunofluorescence of PlexA1 in growth cones and somas of dissociated cortical neurons treated with or without BoNT/D and/or Sema3A. Bars, 4 µm.

Published January 2, 2012

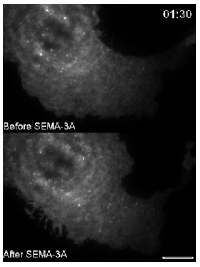


Video 1. **Sema3A treatment decreases rate of Syb2-SEP exocytosis in Cos7 cells.** Cos7 cells transfected with PlexA1-FLAG, Nrp1-mRFP, and Syb2-SEP were recorded for Syb2-SEP exocytosis events before (top) and after (bottom) treatment with 1 µg/ml Sema3A-Fc. Images were analyzed by time-lapse microscopy using an inverted epifluorescence microscope (DMI6000B; Leica). Frames were taken every 500 ms for 3 min. Note that exocytic events appear as transient flashes of light. Time is indicated in minutes and seconds. Bar, 10 µm.